Journal of the Korean Nuclear Society
Volume 32, Number 5, pp.465~476, October, 2000

Evaluation of Plugging Criteria on Steam Generator Tubes and Coalescence Model of Collinear Axial Through-Wall Cracks

Jin Ho Lee, Youn Won Park, Myung Ho Song
Korea Institute of Nuclear Safety
19 Kusong, Yusong, Taejon 305-338, Korea
s012ljh@kins.re.kr

Young Jin Kim, Seong In Moon
Sungkyunkwan University
300 Chunchun, Jangan, Suwon 440-746, Korea

(Received Faburury 21, 2000)

Abstract

In a nuclear power plant, steam generator tubes cover a major portion of the primary pressure-retaining boundary. Thus very conservative approaches have been taken in the light of steam generator tube integrity. According to the present criteria, tubes wall-thinned in excess of 40% should be plugged whatever causes are. However, many analytical and experimental results have shown that no safety problems exist even with thickness reductions greater than 40%. The present criterion was developed about twenty years ago when wear and pitting were dominant causes for steam generator tube degradation. And it is based on tubes with single cracks regardless of the fact that the appearance of multiple cracks is more common in general.

The objective of this study is to review the conservatism of the present plugging criteria of steam generator tubes and to propose a new coalescence model for two adjacent through-wall cracks existing in steam generator tubes. Using the existing failure models and experimental results, we reviewed the conservatism of the present plugging criteria. In order to verify the usefulness of the proposed new coalescence model, we performed finite element analysis and some parametric studies. Then, we developed a coalescence evaluation diagram.

Key Words : coalescence criterion, interaction effect, steam generator tube, plastic collapse, plugging, rupture

1. Introduction

The heat transfer area of the steam generators in a pressurized water reactor can comprise well over 50% of the total primary pressure-retaining boundary. The steam generator tubing, therefore,

represents an integral part of a major barrier against fission product release to the environment. It is commonly required that tubes with defects exceeding 40% of wall thickness in depth should be plugged[1,2]. However, this criterion is considered to be too conservative for some locations and types of defects because many analytical results show that the integrity of steam generator tubes, locally thinned or cracked, could still be maintained under normal operations and even during postulated accident conditions[3,4].

As a practical approach, the U.S. Nuclear Regulatory Commission (USNRC) allows licensees to develop and implement steam generator defect specific management (SGDSM) strategies provided that the structural and leakage integrity of tubes are ensured. Many studies have been done to develop alternative plugging criteria and have shown that a certain range of axial through-wall cracks in steam generator tubes could remain in service without safety or reliability problems[3~5]. One of limitations of these approaches is that they are based on tubes with single cracks, and so their failure analyses are carried out using an idealized single crack to reduce complexity. However, test results of removed steam generator tubes[6] and in-service inspection results show that the formation of multiple cracks is the general case[7].

If a circumferential crack is detected, the concerned tube is normally plugged whatever the length is because the circumferential crack isn' t usually detected until it propagates up to greater than 50% in thickness. In terms of plugging criteria development, therefore, the axially cracked tube is more meaningful in practice. And multiple axial cracks could be handled by the combination of two components: collinearly oriented and circumferentially spaced. The former could be more easily handled in view of a development of coalescence criterion, so that it was taken first.

In this paper, the conservatism of the present plugging criteria of steam generator tubes is reviewed and a new coalescence model for two adjacent through-wall cracks is proposed. Using the existing failure models and experimental results, we reviewed the conservatism of the present plugging criteria. In order to verify the usefulness of the proposed new coalescence model, we performed finite element analysis. Some parametric studies were also carried out to investigate effects of flow stress and stress-strain curve on the coalescence behavior of the adjacent cracks. Then, we developed a coalescence evaluation diagram, which could be used to determine whether the adjacent cracks detected by nondestructive evaluation (NDE) coalesced with each other or not. Once two cracks are determined to be coalesced, they can be considered to be an equivalent single crack.

2. Conservatism of Present Plugging Criteria

In order to determine the analysis method for steam generator tubes, Yu et al.[4] used the R6 approach developed by the Central Electricity Generating Board (CEGB). This approach uses K_r and L_r as variables. K_r is the ratio of the elastically calculated stress intensity factor to the fracture toughness of the material. L_r is the ratio of the nominal stress in the component to the yield strength of the material. The failure assessment curve is given as follows:

$$K_r = (1-0.14L_r^2)\{0.3+0.7\exp(-0.65L_r^6)\} \quad (1)$$

This failure assessment curve and the applied K_r and L_r values for a given loading condition are plotted in Fig. 1 for various crack lengths. The material properties and geometry of the steam generator tubes of Ulchin #1 (Korea, Framatome type PWR) were used in this analysis. The applied K_r and L_r values lie in the region of $K_r/L_r < 0.2$.

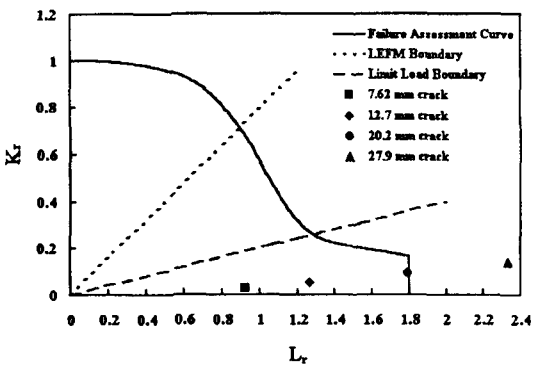

Fig. 1. Failure Assessment Diagram

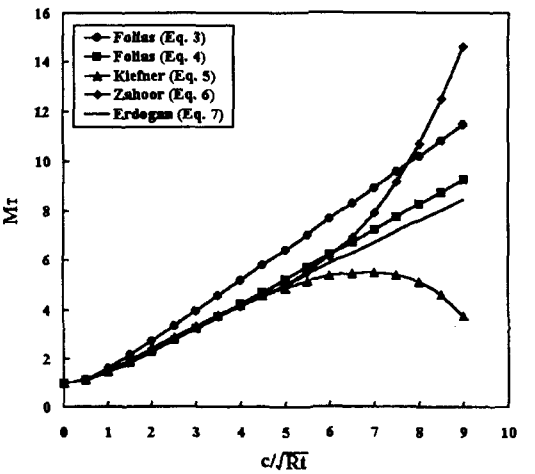

Fig. 2. Bulging Factor for Different Cases

Therefore, the failure mode is plastic collapse and limit load analysis can be used to assess the failure of steam generator tubes.

2.1. Limit Load Analysis

The pressure necessary to cause unstable ductile (plastic collapse) failure of tubes with an axial through-wall crack, P_{cr}, is calculated using Eq. (2).

$$P_{cr} = \frac{\sigma_f t}{M_T R} \tag{2}$$

where σ_f is the flow stress, t is the wall thickness, MT is the bulging factor, and R is the mean radius of the tube. In Eq. (2), the accuracy of the failure pressure depends on M_T because all the other factors are set to be constant for a given tube. Several expressions for M_T were proposed as shown below[8~12]:

$$M_T = [1 + 1.61(c/\sqrt{Rt})^2]^{0.5} \quad \text{for } \lambda \le 2 \tag{3}$$

$$M_T = [1 + 1.05(c/\sqrt{Rt})^2]^{0.5} \quad \text{for } R/t \ge 10 \tag{4}$$

$$M_T = [1 + 1.255(c/\sqrt{Rt})^2 - 0.0135(c/\sqrt{Rt})^4]^{0.5} \quad \text{for } \lambda \le 9 \tag{5}$$

$$M_T = [1 + 1.2987(c/\sqrt{Rt})^2 - 0.026905(c/\sqrt{Rt})^4 + 0.00053549(c/\sqrt{Rt})^6]^{0.5} \quad \text{for } c/\sqrt{Rt} \le 5 \tag{6}$$

$$M_T = 0.614 + 0.481\lambda + 0.386\exp(-1.25\lambda) \quad \text{for } 5 \le R/t \le 50 \tag{7}$$

where $2c$ is the axial crack length and λ is the shell parameter defined by Eq. (8). Among these equations, Eq. (7) is widely used and Fig. 2 shows its usefulness. In this paper, Eq. (7) is used to calculate the failure pressure of the tube with a single through-wall crack.

$$\lambda = [12(1-\nu^2)]^{0.25}(c/\sqrt{Rt}) \tag{8}$$

For axial part-through cracks, the pressure required to fail the remaining ligament, P_{sc}, can be calculated from an empirical equation reported by Kiefner et al.[10].

$$P_{sc} = \frac{\sigma_f t}{M_P R} \tag{9}$$

where

$$M_P = \frac{1 - \dfrac{a}{M_T t}}{1 - \dfrac{a}{t}}$$

In Eq. (9), a is the crack depth, M_P is the magnification factor for the part-through crack, and M_T is the same bulging factor as used in the through-wall cracks except that $2c_{eq}$ is used instead of $2c$. When A indicates the area of the part-

through crack, $2c_{eq}$ is defined as $2c_{eq} = A/a$. The stability of the resulting through-wall crack can be analyzed by solving Eq. (2). If $P_{cr} > P_{sc}$, the through-wall crack is stable. Although the crack will leak, it will not increase in length without a further increase in pressure. If $P_{cr} < P_{sc}$, the resulting crack will be unstable and will rapidly increase in length without any additional increase in pressure.

Under the auspices of a NRC-sponsored steam generator integrity program, PNNL conducted a series of tests on tubes that contained part-through axial slots[13]. Based on these tests, ANL developed an empirical equation for the ligament failure pressure of a tube that contained an axial part-through crack[14]. The equation is of the same form as Eq. (9) except that M_P of Eq. (9) is replaced by

$$M_P = \frac{1-\alpha\frac{a}{M_T t}}{1-\frac{a}{t}} \qquad (10)$$

where

$$\alpha = 1 + 0.9\left(\frac{a}{t}\right)^2\left(1-\frac{1}{M_T}\right)$$

In Eq. (10), α is the parameter dependent on a/t. Eq. (10) predicts the ligament failure pressures similar to those predicted by Eq. (9) but the latter tends to be overly conservative for shallow and deep cracks[14]. In this paper, therefore, we adopted Eq. (10), which covers all range of crack depth.

Fig. 3 shows the failure pressures obtained from Eq. (2) and (10) for the through-wall cracked tube and for the part-through cracked tube of a/t = 0.4 as a function of the axial crack length. In this figure, burst test results of through-wall cracked tubes are also plotted for comparison. The open circles indicate burst test results carried out under various pressurization rates by Framatome[15]. The solid triangles indicate temperature-compensated burst test results, which were performed at the pressurization rate of 13.8MPa/s by Argonne National Laboratory[16]. On the basis of the 40% of wall criterion, the part-through crack of a/t = 0.4 was selected. The material properties, geometry, and operating conditions of the steam generator tubing of Ulchin #1 were used in calculating the failure pressures and were summarized in Table 1. The definition of the flow stress given in Eq. (11) was used and its value was derived from the lower bound value in the CMTR of the steam generator tubes of Ulchin #1[17].

$$\sigma_f = k(\sigma_{YS} + \sigma_U) = 0.5(\sigma_{YS} + \sigma_U) \qquad (11)$$

where k is the flow stress factor, σ_{YS} is the yield strength and σ_U is the ultimate tensile strength. The safety factors of 3 and 1.4 are considered for normal operation and accidential condition, respectively, in accordance with requirements of Regulatory Guide 1.121[1]. Considering these factors, we can obtain 30.6MPa as a maximum pressure which occurs in the steam generator tubes of Ulchin #1.

As shown in Fig. 3, burst test results are well

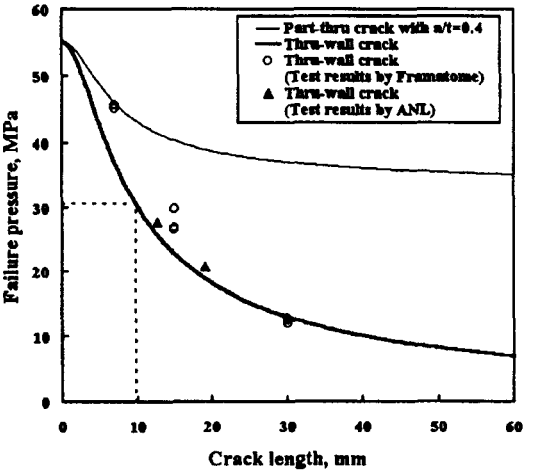

Fig. 3. Limit Load Solutions for Through-wall and Part-through Crack

Table 1. Specification of Ulchin #1 Steam Generator Tubes

Outer Diameter	22.2 mm
Thickness	1.27 mm
Material	Inconel Alloy 600TT
Young' s Modulus at 300℃	199.8 GPa
Yield Strength at 300℃	256.0 MPa
Tensile strength at 300℃	656.0 MPa
Flow Stress at 300℃	456.0 MPa
Pressure across the wall at Normal Operation	10.2 MPa
Pressure across the wall at Accident Condition	18.3 MPa

bounded by the predicted failure pressure curve for the through-wall crack. It is noted that the through-wall cracked tube fails at the crack length of 9.8mm but the part-through cracked tube never fails regardless of crack length. Therefore, there is no problem in the structural integrity of steam generator tubes whenever the crack depth is less than 40% of the wall thickness. This means that the current plugging criteria based on 40% wall thickness could be justified regardless of crack length. But this criterion is considered to be too conservative especially for axial cracks of less than 9.8mm in length because the steam generator tube with a single through-wall crack of less than 9.8mm maintains its structural integrity in the event of the foregoing maximum pressure as shown in Fig. 3. In addition, most of the detected cracks are located in the roll transition zone. In this case, the tube sheet constrains the deformation of the tube and shares the applied loads. It is too conservative to apply the 40% of wall criterion for all cases without considering location or length. Besides, it is so difficult to measure the depth of a detected part-through crack reliably using the present NDE techniques. It is, therefore, necessary to develop alternative criteria on the basis of SGDSM strategies. To accomplish this goal, many works have been done. But these approaches have been limited to tubes with a single crack whereas multiple cracks are found more frequently[6,7].

3. Coalescence Model

In this chapter, we reviewed the present coalescence criteria for multiple surface cracks and proposed a new coalescence model for the collinear axial through-wall cracks existing in steam generator tube.

3.1. Present Coalescence Criteria for Collinear Surface Cracks

Until now, several criteria as shown below have been used to determine the onset of the coalescence between two adjacent surface cracks.

- ASME Sec. XI, IWA-3000[18]:
$$\delta_0 = \max(2a_1, 2a_2) \tag{12}$$

- BSI PD 6493[19]: $\delta_0 = c_1 + c_2$ (13)

- Coalescence of surface points: $\delta_0 = 0$ (14)

where δ_0 is the distance between two adjacent surface cracks at the onset of coalescence, a_1 and a_2 are the crack depths, and c_1 and c_2 are the half crack lengths. Of these equations, it is known that Eq. (14) shows a good agreement with the experimental results[20~22]. This means that two adjacent cracks coalesce when there is no remaining ligament between them, i.e., immediately after the ligament between the adjacent cracks can no longer sustain the applied loads. However, these three criteria were developed for the application to pressure vessels and pipings whose failure behavior is quite

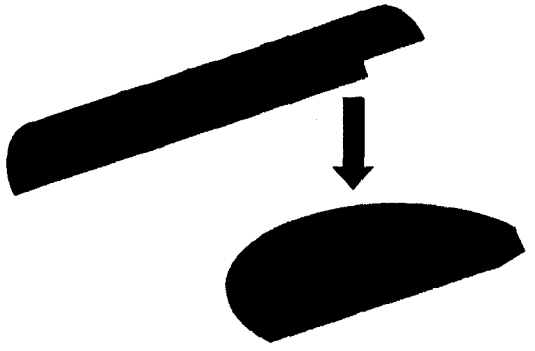

Fig. 4. Finite Element Mesh of Steam Generator Tube

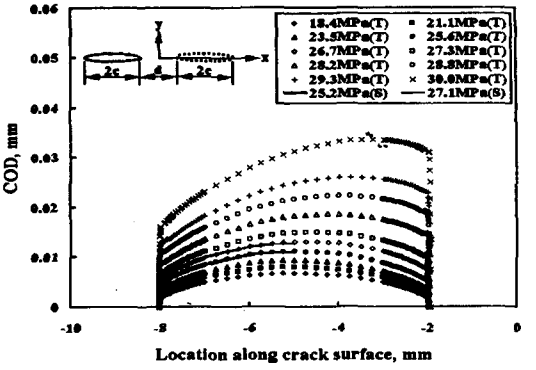

Fig. 5. Change of Crack Opening Displacement

different from steam generator tubes.

As discussed before, the failure behavior of cracked steam generator tubes is dominated by large scale yielding. Therefore it is necessary to develop a new criterion applicable to the case of large scale yielding.

3.2 Coalescence Model for Collinear Axial Through-wall Cracks

Unlike the case of small scale yielding, δ_0 depends on the plastic zone size in large scale yielding, and thus becomes a function of the geometry, crack size, and applied loads as follows:

$$\delta_0 = f\left(\frac{c}{\sqrt{Rt}}, \frac{a}{c}, \frac{P_i}{P_{sc}}\right) \quad (15)$$

where P_i is the applied pressure. In the case of through-wall cracks, Eq. (15) can be arranged like Eq. (16).

$$\delta_0 = f\left(\frac{c}{\sqrt{Rt}}, \frac{P_i}{P_{cr}}\right) \quad (16)$$

As described before, the failure of a steam generator tube containing a crack can be predicted using the limit analysis, which assumes that a given material behaves in an elastic-perfectly plastic manner and its yielding takes place at the flow stress. In this study, it is assumed that the ligament between two adjacent cracks can' t sustain the applied loads any more when it is subject to the fully yielding condition. Therefore, it is possible to establish this condition as a new crack coalescence criterion applicable to the steam generator tube with collinear axial through-wall cracks.

4. Coalescence Evaluation Diagram

4.1. Finite Element Analysis

In order to verify the suggested coalescence criterion applicable to the steam generator tube with collinear axial through-wall cracks, elastic-plastic finite element analysis was performed using ABAQUS. The material properties and geometry of the steam generator tubing of Ulchin #1 were used. And it is assumed that this material behaves in an elastic-perfectly plastic manner with a flow stress of σ_f. Fig. 4 shows the finite element mesh of the steam generator tube. A quarter of the tube was modeled using the symmetry and isoparametric 20-node reduced-integration brick elements were used. The axial crack length, $2c$, is 6mm and the distance between the cracks, d, is 4mm. As the pressure increases progressively, the

changes in crack opening displacement (COD), stress distribution and plastic zone were observed in the mid-plane of the wall thickness.

Another set of analyses was performed to create a diagram, which can be used to determine whether the adjacent cracks detected by NDE coalesce or not. For the various crack lengths and distances between the cracks, we determined the applied pressures when the ligament is subjected to the fully yielding condition. The diagram, called a coalescence evaluation diagram, was established based on these results.

4.2. Coalescence Behavior of Two Axial Cracks

Fig. 5 shows the changes in COD as the pressure increases from 0MPa to 30MPa. In this figure, symbols and solid lines indicate the results for two through-wall cracks and a single through-wall crack, respectively. It is shown that the displacement for the adjacent through-wall cracks increases rapidly after 26.7MPa. This trend is more conspicuous near the inner crack tip than near the outer crack tip. Fig. 6 shows the distributions of the Mises stress in the ligament as the pressure increases. This figure shows that the ligament is fully yielded at 26.7MPa. Fig. 7 shows the changes in plastic zone size in mid-plane as the pressure increases. The plastic zone size of the inner crack tip region is similar to that of the outer crack tip region at 23.5MPa. It increases substantially at 25.6MPa and the ligament is fully yielded at 26.7MPa. In addition, it was observed that the COD and plastic zone size on the inner and outer wall surfaces increase rapidly after 26.7MPa.

From the above results, it can be seen that the rapid changes in COD and plastic zone size take place immediately after the ligament between the cracks is fully yielded. These changes take place because the ligament can no longer sustain the applied loads after fully yielding. Once the adjacent cracks come together, they are considered to be a single equivalent crack, i.e., $2C_{new} = 2C + d + 2C$.

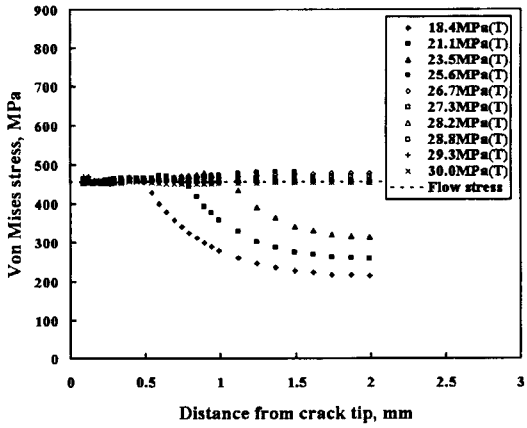

Fig. 6. Distribution of Von Mises Stress

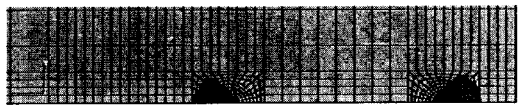

(a) P_i = 23.5MPa

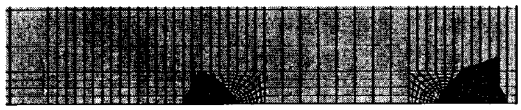

(b) P_i = 25.6MPa

(c) P_i = 26.7MPa

Fig. 7. Change in Plastic Zone Size as Pressure Increases

4.3. Coalescence Evaluation Diagram

From the finite element analyses, we created the diagram shown in Fig. 8, which could be used to

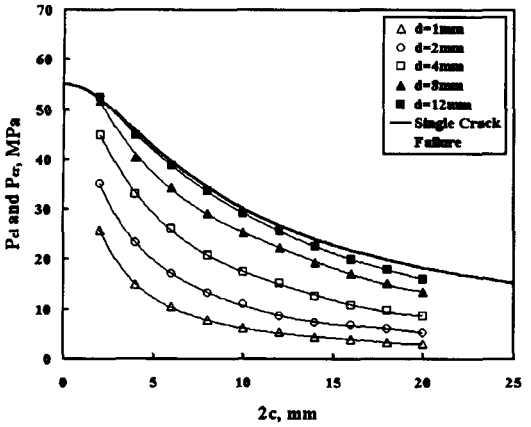

Fig. 8. Coalescence Pressure

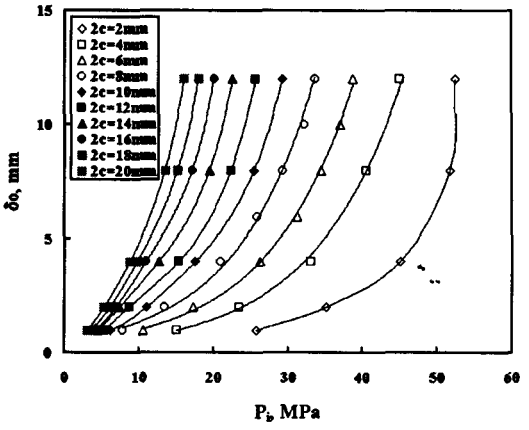

Fig. 9. Coescence Evaluation Diagram

determine the pressure, P_{cl}, at the moment of crack coalescence. In this figure, the thick solid line indicates the failure pressure of the tube with a single crack. Each symbol and its regression line indicate the pressure at the moment of crack coalescence. This figure shows that the coalescence pressure decreases as the crack length increases under the condition of a constant d and increases as the ligament size between cracks increases under the condition of a constant crack length. It is noted that the coalescence pressure for two adjacent cracks with a value of d greater than 12mm closely approaches to the failure pressure of a single crack.

This means that the interaction effect between two adjacent cracks disappears when the ligament length exceeds 12mm for the present model.

The parameter d in Fig. 8 can be replaced with δ_0 which is the value at the onset of crack coalescence. By changing the coordinate system of Fig. 8, Fig. 9 can be obtained which is named a coalescence evaluation diagram. Using Fig. 9, it can be determined whether the adjacent cracks detected by NDE coalesce under a given pressure. Once the adjacent cracks coalesce, they can be considered as a single crack with equivalent length, $2C_{new} = 2C + d + 2C$. This newly defined crack will be used for making decision of plugging the associated tube: the tube should be plugged if a tube failure could occur under the maximum pressure determined with a safety factor for all service level loadings.

5. Parametric Studies

Parametric studies were carried out to investigate effects of flow stress and stress-strain curve on the coalescence pressure.

5.1. Effect of Flow Stress

The value of $k = 0.5$ was used to determine flow stress in the previous chapters. However the k value for Alloy 600, as reported in the literature, usually varies between 0.5 and 0.6[14,23,24]. To investigate effects of flow stress on coalescence pressure, finite element analyses using $k = 0.55$ were performed and the results were plotted in Fig. 10. This figure shows a similar trend to that of Fig. 8 obtained using $k = 0.5$: the coalescence pressure for the adjacent cracks having the value of d greater than 12mm is bounded by the failure

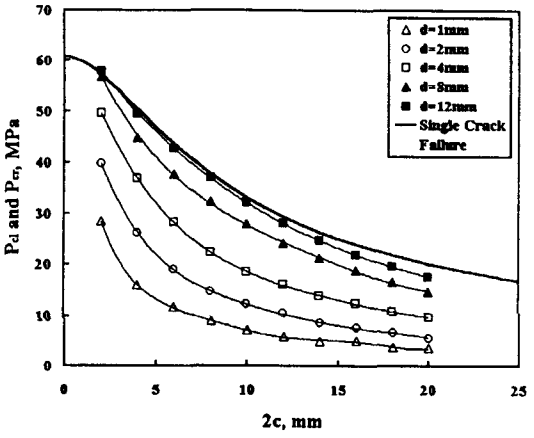

Fig. 10. Coalescence Pressure (k = 0.55)

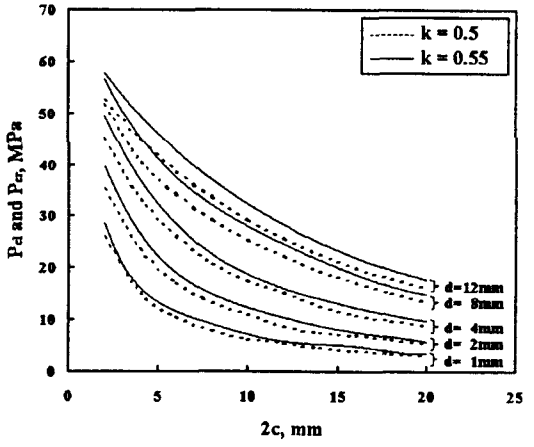

Fig. 11. Comparison of Coalescence Pressures Obtained from Different *k* Values

pressure of a single crack. Therefore, for steam generator tubes with the material specifications given in Table 1, it can be concluded that the interaction effect between two adjacent cracks disappears as the ligament length exceeds 12mm.

Fig. 11 shows the comparison of coalescence pressures obtained from two k values. As expected the results obtained using k = 0.55 give higher coalescence pressures than those obtained using k = 0.5. The average difference between two results is 11%. That is, a ten percent higher k value produces about ten percent higher coalescence pressure.

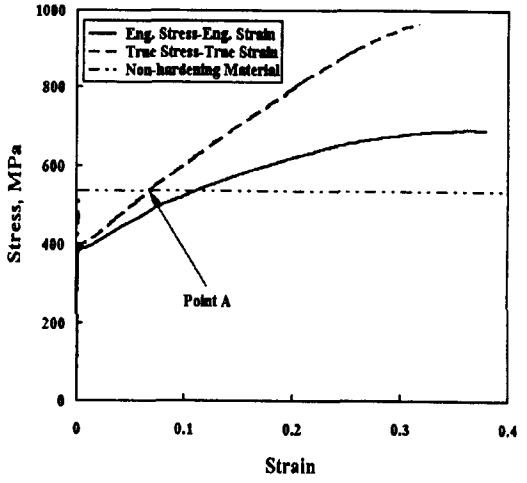

Fig. 12. Stress-strain Curve for 22.2mm-diameter Alloy 600 Tube at Room Temperature[24]

As k is a certain value due to the manufacturing process, the heat treatment condition, aging of tubes and so on, linear interpolation can be made to determine the coalescence of the adjacent cracks.

5.2. Effect of Stress-strain Curve

It is necessary to investigate the behavior of a real material showing strain hardening because the present model assumes that the given material behaves in an elastic-perfectly plastic manner with a yielding value of σ_f. In order to investigate the influence of strain hardening on crack coalescence, finite element analyses were performed using the full stress-strain curve of Fig. 12. Young's modulus is 213GPa[25], the yield strength is 379MPa, and the tensile strength is 690MPa[24] for this material. Two collinear axial through-wall cracks were modeled and the crack shape of $2c$ = 10mm and d = 2mm was used.

Fig. 13 shows the COD changes for the

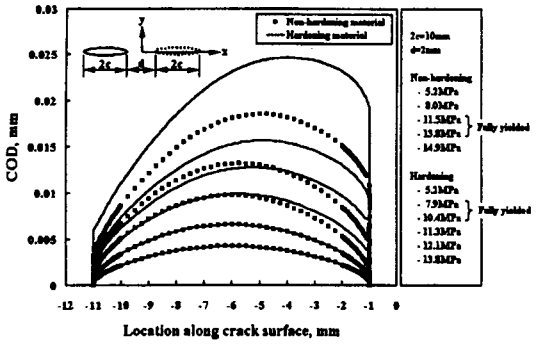

Fig. 13. Comparison of COD's Between Non-hardening and Hardening Materials at Early Loading Stage

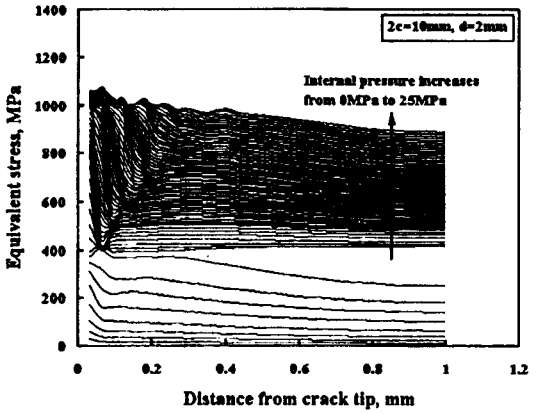

Fig. 14. Crack Tip Stress Fields for Hardening Material

hardening material and for the non-hardening material with k = 0.5. For the non-hardening material, the ligament between the adjacent cracks was fully yielded between 11.5MPa and 13.8MPa. And the ligament was fully yielded between 7.9MPa and 10.4MPa for the hardening material. Before the fully yielding condition in the hardening material is reached, COD values of the hardening material and non-hardening material are almost same. Above this, COD values of the hardening material increase more rapidly than that of non-hardening material.

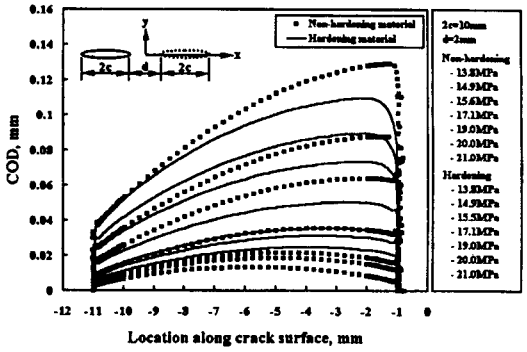

Fig. 15. Comparison of COD's Between Non-hardening and Hardening Material at High Loading Stage

Fig. 14 shows the equivalent stress distribution along the ligament for hardening material. After the stresses in the ligament exceed the yield strength of 379MPa and the ligament is fully yielded, no distinguishable stress gradient is observed until about 800MPa except the crack tip region. This trend explains why yield strength plays an important role on the crack coalescence.

As shown in Fig. 12, the crack tip of the hardening material approaches to an earlier yield point compared to that of the non-hardening material. Therefore, the COD at the early loading stage is greater in the hardening material than in the non-hardening material and the behavior is reversed when strain exceeds point A. The COD changes of the hardening and the non-hardening material are shown in Fig. 15. At the early loading stage, COD of the hardening material is greater than that of the non-hardening material. At the high loading stage, however, the COD is reversed.

6. Conclusions

From the study on plugging criteria for steam generator tubes and coalescence behavior of axial through-wall cracks, the following conclusions

were obtained.

(1) The conservatism of the present plugging criterion for steam generator tubes was reviewed and it is concluded that the criterion is too conservative for some locations and types of defects.

(2) The steam generator tubes with an axial through-wall crack less than 9.8mm can maintain its integrity under not only normal operation but also accident condition.

(3) A new crack coalescence criterion applicable to the steam generator tube with collinear axial through-wall cracks was proposed and was verified through finite element analysis.

(4) A coalescence evaluation diagram for the steam generator tube was generated. And it can be used to determine whether the adjacent cracks detected by NDE coalesce under the given operating condition.

(5) The selection of an appropriate flow stress is important.

References

1. USNRC, "Bases for Plugging Degraded PWR Steam Generator Tubes," *USNRC*, Regulatory Guide 1.121 (1976).
2. ASME, "Rules for Construction of Nuclear Power Plant Components," *ASME*, ASME Boiler and Pressure Vessel Code, Sec. III (1998).
3. B. Cochet and B. Flesch, "Crack Stability Criteria in Steam Generator Tubes," *9th Int. Conference on SMiRT*, Vol. D, pp.413-419 (1987).
4. Y. J. Yu, J. H. Kim, Y. Kim, and Y. J. Kim, "Development of Steam Generator Tube Plugging Criteria for Axial Crack," *ASME PVP*, Vol. 280, pp.79-83 (1994).
5. J. A. Gorman, J. E. Harris, and D. B. Lowenstein, "Steam Generator Tube Fitness-for-Service Guidelines," *AECB, AECB* Report No. 2.228.2 (1995).
6. J. S. Kim et al., "Investigation Report of Steam Generator Tubes Pulled out from Ulchin #1," *KAERI*, October (1999).
7. S. C. Kang et al., "Regulatory Technical Report on the Steam Generator Safety of Nuclear Power Plants," *KINS*, KINS/AR-669, April (1999).
8. E. S. Folias, "An Axial Crack in a Pressured Cylindrical Shell," *International Journal of Fracture Mechanics*, Vol. 1, pp.104-113 (1965).
9. E. S. Folias, "On the Fracture of Nuclear Reactor Tubes," *3rd Int. Conference on SMiRT*, London, UK, Paper C4/5 (1975).
10. J. F. Kiefner, W. A. Maxey, R. J. Eiber, and A. R. Duffy, "Failure Stress Levels of Flaws in Pressurized Cylinders," *ASTM STP536*, pp.461-481 (1973).
11. A. Zahoor, "Ductile Fracture Handbook Vol. 2, Axial Through-Wall Crack," *EPRI*, EPRI Report NP-6301-D (1989).
12. F. Erdogan, "Ductile Failure Theories for Pressurized Pipes and Containers," *International Journal of PVP*, Vol. 4 (1976).
13. J. M. Alzheimer, R. A. Clark, C. J. Morris, and M. Vagins, "Steam Generator Tube Integrity Program Phase I Report," *USNRC*, NUREG/CR-0718, PNL-2937, September (1979).
14. S. Majumdar, W. J. Shack, D. R. Diercks, K. Mruk, J. Franklin, and L. Knoblich, "Failure Behavior of Internally Pressurized Flawed and Unflawed Steam Generator Tubing at High Temperatures-Experiments and Comparison with Model Predictions," USNRC, *NUREG/CR-6575*, ANL-97/17, Mach (1998).
15. B. Cochet, "Ulchin #1: Answer to the requisitions of KINS," Private Letter from B.

Cochet in FRAMATOME to J. H. Hong in KEPCO, April 16 (1993).

16. D. R. Diercks, "Steam Generator Integrity Program," *ANL*, Steam Generator Tube Integrity Program Monthly Report, March 23 (1999).
17. Framatome, "Certified Material Test Report for Steam Generator Tubes of Ulchin #1," *Framatome* (1983).
18. ASME, "Rules for Inspection and Testing of Components of Light Water Cooled Plants," ASME, ASME Boiler and Pressure Vessel Code, Sec. XI (1998).
19. PD 6493:1980, "Guidance on Some Methods for the Derivation of Acceptance Levels for Defects in Fusion Welded Joints," British Standards Institution, March (1980).
20. Y. J. Kim, Y. S. Choy, and J. H. Lee, "Development of Fatigue Life Prediction Program for Multiple Surface Cracks," *ASTM STP 1189*, pp.536-550 (1993).
21. K. Shibata, N. Yokoyama, T. Ohba, T. Kawamura, and S. Miyazono, "Growth Evaluation of Fatigue Cracks from Multiple Surface Flaws (I)," *Journal of Japanese Nuclear Society*, Vol. 27, No. 3, pp.250-262 (1985).
22. K. Shibata, N. Yokoyama, T. Ohba, T. Kawamura, and S. Miyazono, "Growth Evaluation of Fatigue Cracks from Multiple Surface Flaws (II)," *Journal Japanese Nuclear Society*, Vol. 28, No. 3, pp.258-265 (1986).
23. D. R. Diercks, S. Bakhtiari, K. E. Kasza, D. S. Kupperman, S. Majumdar, J. Y. Park, W. J. Shack, "Steam Generator Tube Integrity Program," *USNRC*, NUREG/CR-6511, Vol. 3, ANL-98/7, August (1998).
24. D. R. Diercks, S. Bakhtiari, K. E. Kasza, D. S. Kupperman, S. Majumdar, J. Y. Park, W. J. Shack, "Steam Generator Tube Integrity Program," *USNRC*, NUREG/CR-6511, Vol. 4, ANL-98/15, January (1999).
25. S. R. Hong et al., "Development of a Crack Growth Analysis Program for Reactor Vessel Head Penetration," *KEPRI*, KEPRI-94Z-J12, August (1996).